OS41C-1572

Eastern and Western Boundary Currents in the Labrador Sea, 1995-2008

Melinda M. Hall[1], Daniel J. Torres[1], Igor Yashayaev[2]

[1]Woods Hole Oceanographic Inst., Woods Hole, MA, United States • [2]Fisheries and Oceans Canada, Bedford Inst. of Oceanography, Dartmouth, NS, Canada

Introduction

In this work, we present estimates of boundary current transports computed from LADCP observations for a sampling of AR7W sections from 1995 through 2008. Boundary currents constitute an important part of the meridional overturning circulation, as they are the conduit for transporting ventilated waters of the northern seas out into the Atlantic. In recent decades, intensive observational efforts in the Labrador Sea have led to a clearer picture of the circulation in that basin; among these efforts is the annual occupation of the hydrographic line designated AR7W, which has included LADCP data almost every year since 1995. We have previously presented results discussing the section-wide circulation for particular years, comparison with geostrophic velocities, and heat flux as determined from individual as well as composite sections. Figure 1 shows the location of AR7W in the Labrador Sea, as well as vector velocities measured by the LADCP (averaged over 0 - 500 m) for all 6 years that we discuss in this poster. Station positions have been projected onto the AR7W line. The boundary currents are robust features that stand out from the more variable – and weaker – flow in the middle of the basin. On the western side, the 0-500 m velocities can be as strong as 40-50 cm/sec, while on the east they are even larger, as much as 60 cm/sec. Note that coverage varies from year to year, an issue that becomes important when trying to assess boundary current transports, and which is discussed in more detail below. The flow has a strong barotropic component, so the vector velocities show in Figure 1 are representative of the top-to-bottom flow as well. The sense of the boundary current circulation is cyclonic: the eastern boundary current (EBC) heads northwestward along the coast of Greenland, while the western boundary current (WBC) flows southeastward along Labrador.

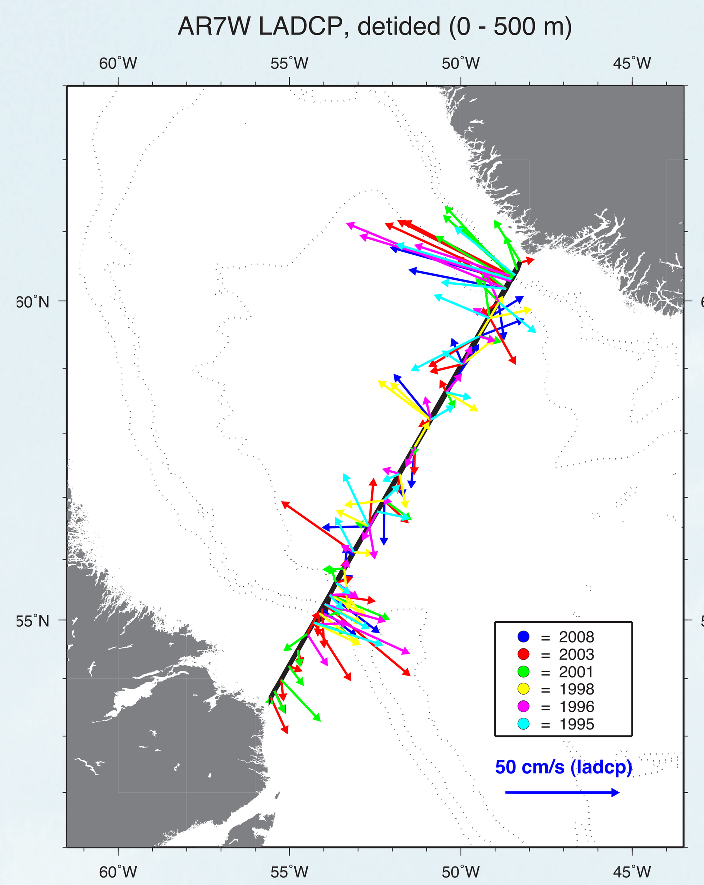

Figure 1: Mean (0 - 500m) detided LADCP velocity vectors for each year indicated.

3

Figure 3 shows a composite velocity section based on the 6 years of LADCP data we examine here. All profiles were lumped together and treated as one dataset, which we then smoothed and mapped the same way as the individual sections. Note that between the boundaries X=43 km and X=728 km, at least 5 of the 6 sections contributed profiles to the composite. We have used the similar 6-year composite of σ_θ (not shown) to compute the layer transports shown in Figure 2 and Table 1.

Lavender et al. (2000) first clarified the presence of recirculating waters offshore of the boundary currents in the Labrador Sea based on a compilation of float data. Pickart and Spall (2007; hereafter PS07)) used the same float data to reference a composite geostrophic velocity section using hydrography from AR7W cruises from 1990-1997. The resulting velocity section contained recirculation gyres with extremely weak speeds, on the order of 1 cm/sec. In contrast, our composite LADCP velocity section shows a somewhat similar pattern, but with much stronger barotropic velocities throughout the basin. Boundary currents in our composite section are narrower than those shown in PS07.

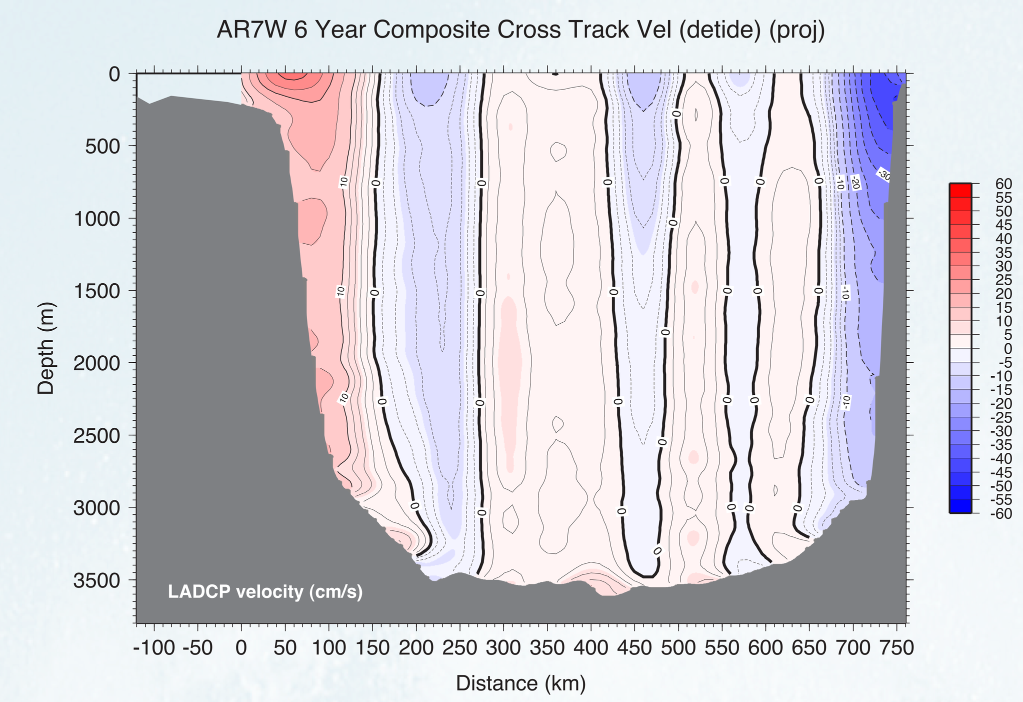

Alternating bands of equatorward (pink, >0) and poleward (blue, <0) velocities transport the following amounts of water (in Sv):

WBC	29.25 (equatorward)
Western Recirculation	-20.38 (poleward)
Central Basin	16.44
400-500 km	-8.64
470-550 km	7.73
530-610 km	- 2.35
580-670 km	4.14 (Eastern Recirculation)
EBC	-37.15

For individual years, reverse flow offshore of the boundary currents may be as strong as those currents themselves. It is thus difficult to interpret our velocity sections and boundary current "throughput" in the same manner as done by PS07.

2

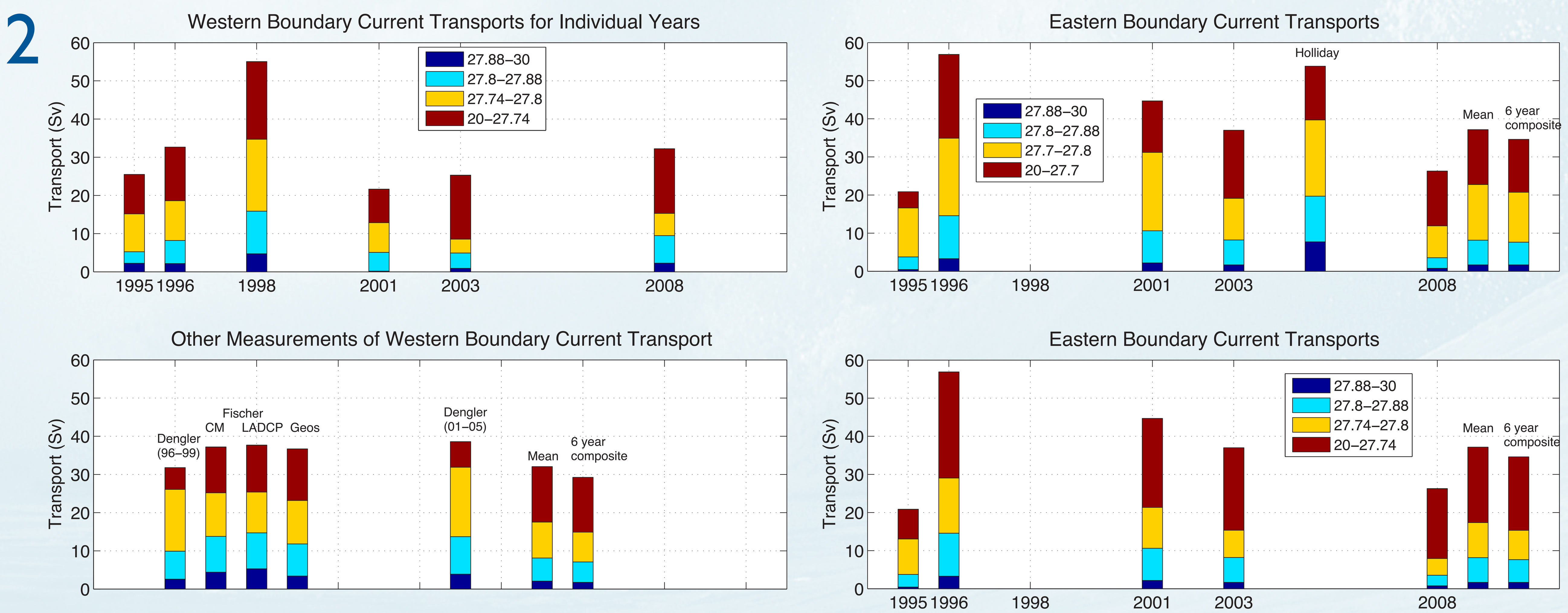

Figure 2 (left): Boundary current transports for the western (left) and the eastern (right) boundaries of AR7W. Transports labeled "mean" and "composite" are derived from the data we discuss here. Other estimates are from Dengler et al. (2006) near 56°N, for measurement periods indicated, based on moored and LADCP data; from Fischer et al. (2004), who present estimates from current meter measurements (1997-1999), and LADCP and geostrophic measurements (1996-2001), near 53°-54°N. Measurements by Holliday et al. (2009) on the eastern side of the Labrador Sea are at about 59°N, using data from Aug.-Sept., 2005. The upper and lower panels for the EBC show different density classes.

To compute transports in the boundary currents or elsewhere along the section, we have first projected the data onto the common AR7W line shown in Figure 1. Velocities are rotated 30 degrees counterclockwise (or 60 degrees clockwise) and we consider the component perpendicular to the AR7W line. We have objectively mapped and gridded the observations to achieve a smooth interpolation scheme and to enable direct comparisons between different years. The smoothing scales are 30 km in the horizontal and 50 m in the vertical. (A smaller horizontal scale would be desirable for the boundary currents, but for many sections the sampling in the interior was too sparse to allow for a smaller smoothing scale.) Likewise, potential density has been mapped in the same way for each year in order to compute transport in specific density classes. We refer to the along-track distance as X: for the purposes of this work, the range of X is 0 – 760 km.

In cases where the data did not reach these limits, we have inserted a uniformly zero velocity profile at X = 0 (or 760) before performing the objective mapping. In this way we hope to minimize the error incurred by missing that part of the boundary current transport. Some idea of the size of such errors can be gleaned from the sections that covered the boundary currents completely (2001 and 2003). For the WBCs, inshore of (X = 40 km; 1000 m isobath; 70 km), about (2; 2-5; 4-7) Sv occurs. For the EBC, transport of about 5 Sv occurs inshore of X=730. The 1000 m isobath is at 739 km and inshore of that we find barely over 1 Sv. **Table 1** indicates each section's limits in terms of our along-track distance X (km).

Figure 2 summarizes the boundary current transports. For the two sections that cover the inner shelf on the west (2001, 2003), we compute transport offshore of X = 0, where X is the along-track distance, because there is a velocity reversal in both sections at that location (see later in poster). Waters over the inner shelf are not considered here. Figure 2 includes transport estimates from other authors for sections that are near ours at either end; additionally, we show estimates based on a composite created from all 6 years (see Figure 3), as well as the mean of the individual estimates. LADCP station spacing in the boundary currents was not always optimal: typically it was 20 km in the WBC, but in 1995, for example, there is a 40 km gap between the westernmost 2 LADCP stations. In the EBC, station spacing was generally closer on account of trying to resolve the flow over the very steep topography there.

Several aspects of our estimates stand out:

- variability dominates the pattern, and it is hard to see any relation between changes in the eastern boundary current and those in the west;
- the mean transport is slightly larger than the composite (this is expected), and for both, transport at all density levels except the shallowest is nearly conserved from the EBC to the WBC; the upper layer carries about 5 Sv more in the EBC;
- comparisons with other estimates are reasonable (especially bearing in mind that the time frames are different), but we consistently find less transport in the densest water (σ_θ> 27.8) than do other studies (see Table 1). This result is puzzling and deserves additional study.

Fischer et al. (2004), using data from a moored array, determined that short-term (i.e., intraseasonal) variability introduced the largest source of uncertainty in their mean flow, with a range of 15 – 35 Sv for σ_θ>27.74. This variability swamps seasonal and interannual variability estimated from satellite data to be O(5-6 Sv) each (Han and Tang, 1999, 2001).

For completeness, Table 1 also shows geostrophic transport in the WBC relative to 1500 dbars for all years discussed here, as well as 1997 and 1999. It ranges from 2.5-4.7 Sv, which compares well with Lazier and Wright's (1993) estimates. We have also estimated boundary current transports using geostrophic shear referenced to the LADCP data, and the results are comparable to what we find using only the LADCP (not shown). One notable difference is that in all cases except the WBC in 2008, geostrophic transports of water with σ_θ>27.8 exceed those based on the LADCP data alone.

	Observation Limits (km)		Deep Transports (Sv)			WBC: Geostrophic
Year	Xmin	Xmax	EBC >27.8	WBC >27.8	Year	Rel. to 1500 db
1995	43	739	3.76	5.26	1995	2.77
1996	18	734	14.58	8.19	1996	4.08
1998	43	658	N/A	15.86	1997	2.92/3.25
2001	-120	762	10.63	5.08	1998	2.28
2003	-120	763	8.2	4.93	1999	2.85/3.07
2008	73	728	3.54	9.47	2001	2.51
Mean			8.14	8.13	2003	4.72
Cmpst			7.64	7.09	2008	3.16/4.57

Table 1: Left to right: Xmin and Xmax are the limits of the LADCP data for each year shown; deep transports are those for σ_θ > 27. 8; geostrophic transports are relative to 1500 dbars for the WBC in the years indicated. Where two estimates are given, it is unclear where the offshore limit occurs.

4

As useful as it is to examine the overall picture we have presented, examining each year individually, and comparing the LADCP derived flow field with the hydrographic properties, reveals a number of interesting features. Here we show the velocity sections for 2001 and 2003 (**Figure 4a, b**) to illustrate two such features. (Unfortunately, LADCP sampling between 300 and 650 km in 2001 was sparse – hence the velocity field there is poorly resolved.)

- In the uppermost part of the WBC's for both sections, we see a dual core of the Labrador Current (LC) expression: inshore is the classic, shallower current; the deep LC lies farther offshore, roughly over the 1500-2000 m isobath. As is obvious from the values of Xmin in Table 1, most sections lacked enough LADCP coverage onshore to pick up this double maximum, which is likely why it doesn't appear in the composite shown in Figure 3. The inner current carries about (1.6 Sv, 3.5 Sv) in (2001, 2003); the deeper current carries 5 Sv in 2001 (down to about 800 m) and 9.2 Sv in 2003 (where it extends deeper, to about 900 m). The double velocity maximum is also reflected in the density contours at the western end of the section (not shown): approaching the coastline, isopycnals shallower than about 1500 m plunge downward beneath the deep expression; they then rise slightly before tending downward once more beneath the inshore LC.
- The eastern ends of these two sections illustrate a bimodality that seems to exist in the current structure at that end. In all years, of course, there is reverse flow offshore of the eastern boundary current, almost by definition. However, the location at which the zero velocity contour occurs alternates between about 680-700 km and about 640-650 km. When the current is tightly confined to the slope, as in 2003 (and also 1995, not shown), there is a distinct, narrow band of return flow just offshore of the boundary current. In other cases, the EBC is wide, and offshore lies a broader (and somewhat weaker) reverse flow. In the composite velocity section, this duality of the velocity structure is reflected in the rather weak return flow that appears offshore of the EBC.

4a

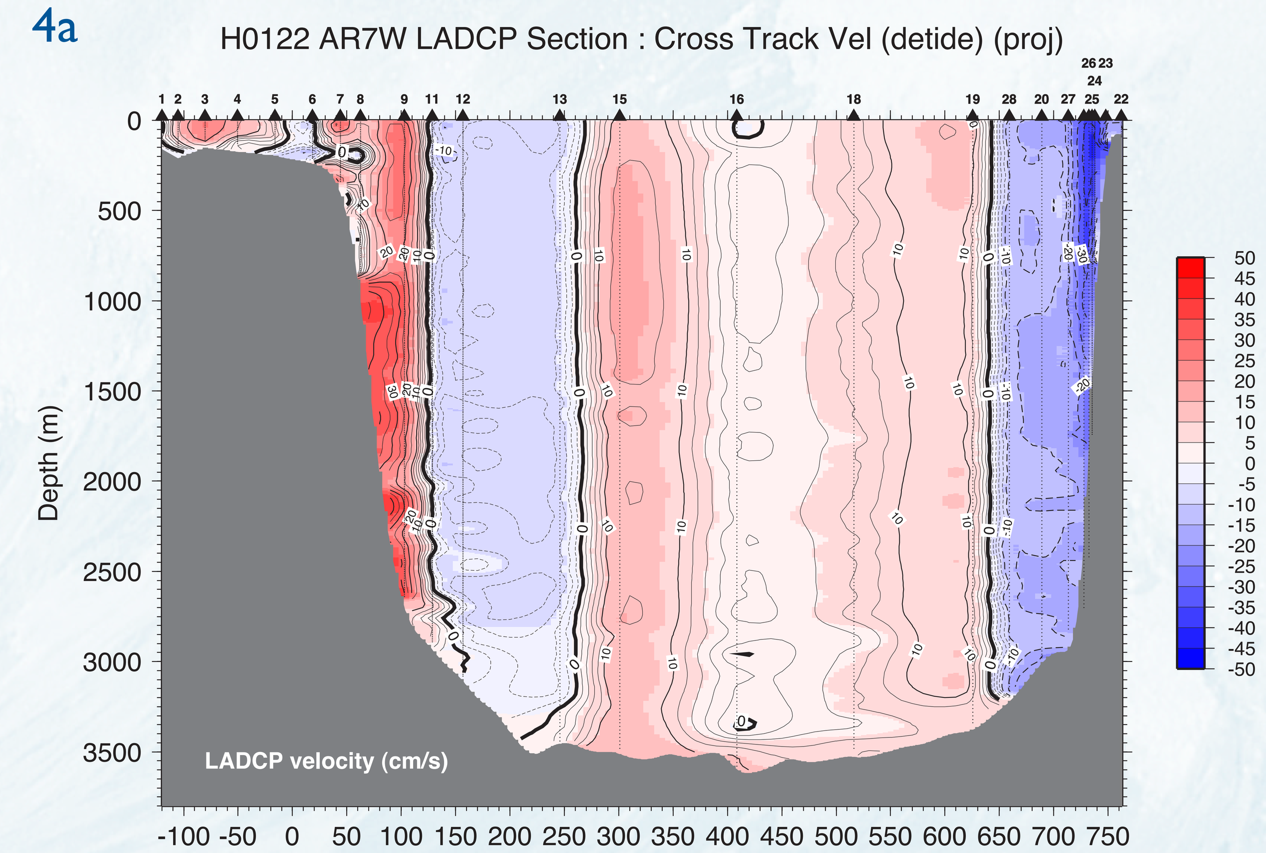

4b

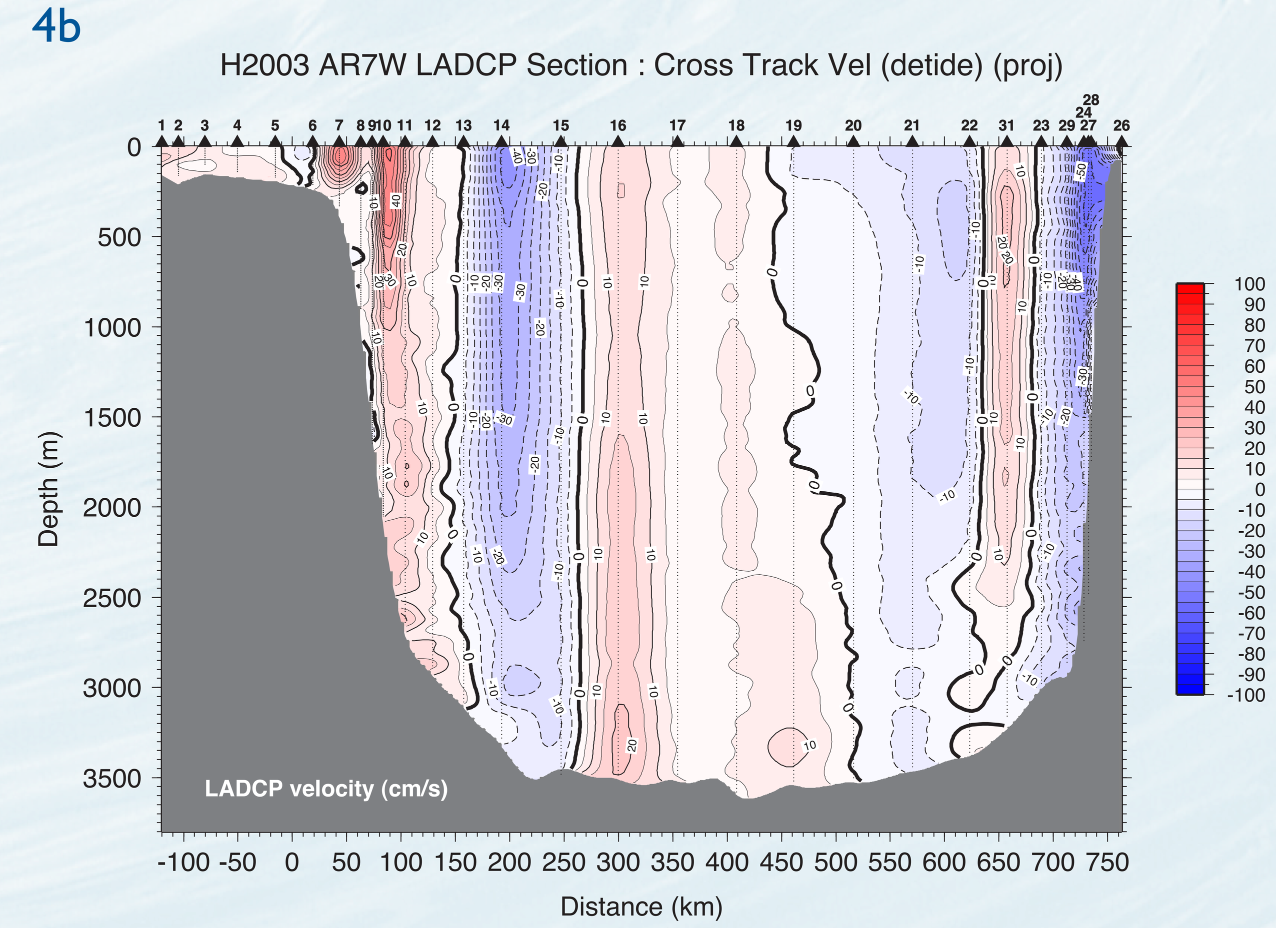

5

Figure 5a shows the location of all Argo profiles used to compute the horizontal gradient of steric height at 10 m depth relative to 1900 m (cm/10 km) as a function of time, shown in **Figure 5b**. All observations have been collapsed onto the AR7W line, and the distance axis in 5b corresponds to the distances shown in the legend of 5a. Each dot on 5b represents a 5-km, 10-day bin containing one or more profiles contributing to the overall picture. Notice that there is only slight overlap in time with the LADCP sections we present here. Nevertheless, this picture reinforces the ideas discussed in this poster: namely, that there is a robust, well-constrained flow on the western side of the Labrador Sea, while the eastern boundary presents a more complex picture, reflecting the bimodality discussed above. For example, in 2002 and early 2003, there is a strong, relatively wide northwestward current off the coast of Greenland, while in late 2006 and early 2007 the northward flow is more constrained horizontally, with a strong velocity reversal immediately offshore of the poleward current. In other years, the currents generally appear to be weaker overall. Thus, although we have only 8 years of these data just now, we can begin to see the alternating pattern on the eastern side. As we process and analyze additional years of LADCP data, perhaps we will see this same pattern emerge, and come to a better understanding of the flow there.

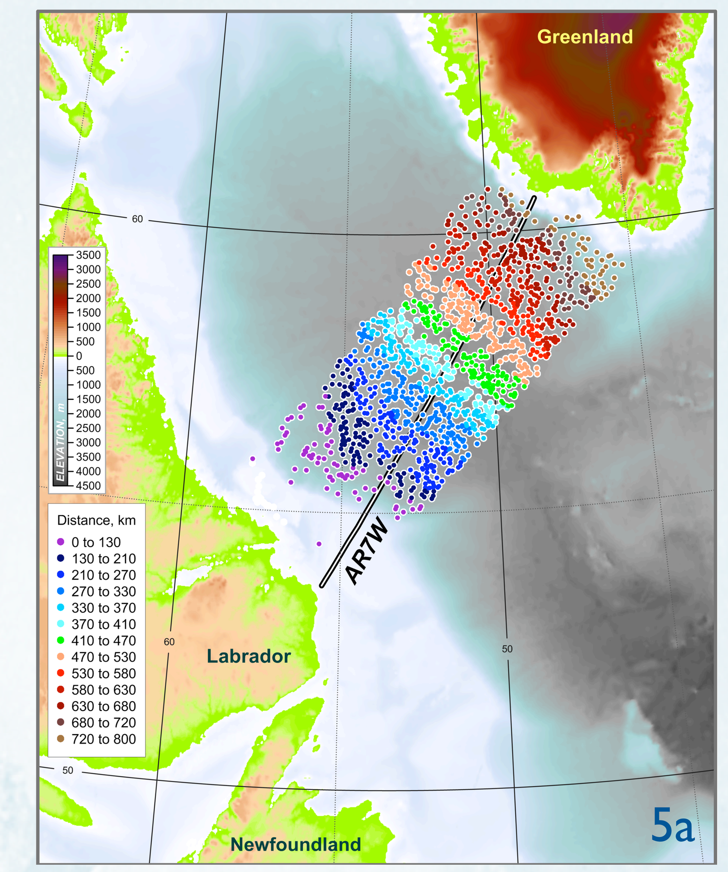

5a

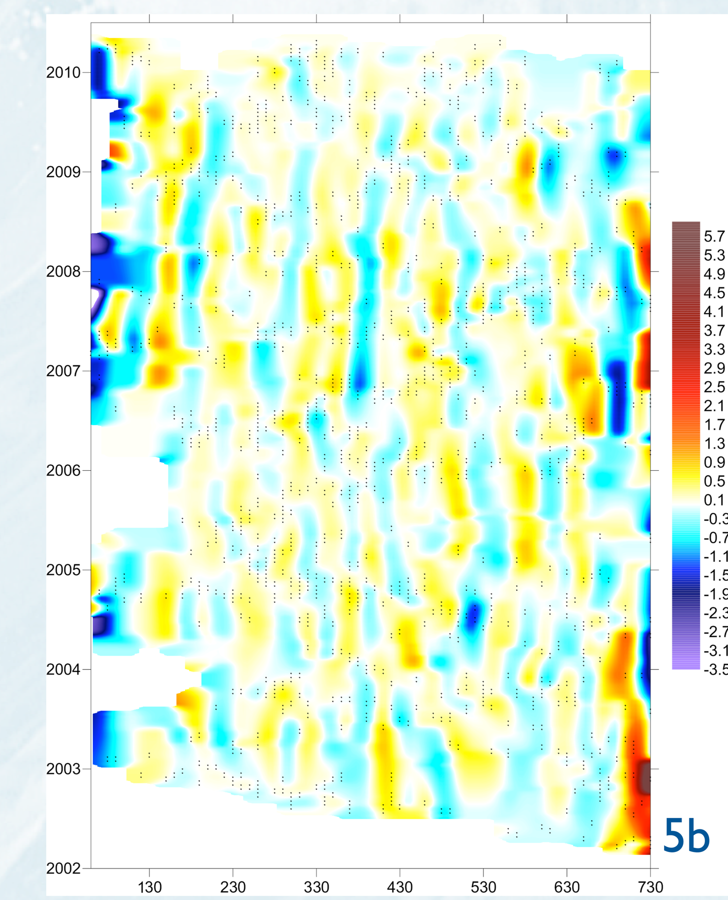

5b

Summary

We have examined the currents on the repeat hydrographic sections crossing the Labrador Sea (AR7W), using LADCP data from 6 occupations of the line. In most cases, we find western and eastern boundary current transports that are comparable to, but typically less than, transports estimated at nearby locations, on both boundaries, by other authors. In particular, we find less transport of overflow waters (σ_θ > 27.8). In the mean, transport in density classes with σ_θ > 27.74 is conserved from the western to eastern boundary; in the lightest layer, the EBC carries an additional 5 Sv.

The western boundary current regime appears to be better defined than the eastern, with a distinct offshore recirculation and a dual core in the LC (Figures 4a, b); adequate data coverage is required to resolve this feature. The circulation near the eastern boundary seems to be bimodal in nature: sometimes the boundary current is more diffuse, with little evidence of a recirculation; at other times, it hugs the boundary and a strong, narrow recirculation occurs immediately offshore. The results deduced from the LADCP velocities are confirmed by Argo data (Figure 5b), for a somewhat different time frame. In the future, by merging more recent LADCP sections with the Argo and remote sensing data, we hope to gain new insight into the nature of the EBC and the relationship of the eastern to the western boundary flow.

Acknowledgments:

We would like to thank the many individuals from the Ocean Sciences Division of Fisheries and Oceans Canada, at the Bedford Institute of Oceanography, whose cooperation has made the collection of the LADCP dataset possible, and who have provided the hydrographic data from their annual survey of the Labrador Sea's AR7W line.

M. Hall and D. Torres have been supported in this work by NSF Grant OCE-0622640.

I. Yashayaev is supported by the ocean climate monitoring program of the Departments of Fisheries and Oceans Canada.

References:

Dengler, M., J. Fischer, F. A. Schott and R. Zantopp (2006), Deep Labrador Current and its variability in 1996-2005, *Geophys. Res. Letters,* **33**, L21S06, doi: 10.1029/2006GL026702.

Fischer, J., F. Schott, and M. Dengler (2004), Boundary circulation at the exit of the Labrador Sea, *J. Phys. Oceanogr.,* **34**, 1548-1570.

Han, G. and C. L. Tang, 1999, Velocity and transport of the Labrador Current determined from altimetric, hydrographic and wind data. *J. Geophys. Res.,* **104**, 18,047-18,057.

Han, G. and C. L. Tang, 2001, Interannual variations of volume transport in the western Labrador Sea based on TOPEX/Poseidon and WOCE data, *J. Phys. Oceanogr.,* **31**, 199-211.

Holliday, N. P., S. Bacon, J. Allen, and E. L. McDonagh (2009), Circulation and transport in the western boundary currents at Cape Farewell, Greenland, *J. Phys. Oceanogr.,* **39**, 1854-1870.

Lavender, K.L., Davis, R.E., Owens, W.B., 2000, Mid-depth recirculation observed in the interior Labrador and Irminger Seas by direct velocity measurements. *Nature,* **407**, 66–69.

Lazier, J. R. N., and D. G. Wright (1993), Annual velocity variations in the Labrador Current, *J. Phys. Oceanogr.,* **23**, 659-678.

Pickart, R. S., and M. A. Spall, Impact of Labrador Sea convection on the North Atlantic meridional overturning circulation, *J. Phys. Oceanogr.,* **37**, doi: 10.1175/JPO3178.1.